

Electronic Supplementary Information (ESI)

Expanding the interlayers of molybdenum disulfide toward the
highly sensitive sensing of hydrogen peroxide

Yijin Shu,^a Wenbiao Zhang,^a Huaihong Cai,^a Yang Yang,^a Xiang Yu^{a,b} and Qingsheng Gao*^a

^a Department of Chemistry, Jinan University, Guangzhou 510632, China. E-mail:
tqsgao@jnu.edu.cn

^b Analytic and Testing Centre, Jinan University, Guangzhou 510632, China

Table S1. Elemental analysis results of MoS₂-based materials investigated in this work.^[a]

Entry	Materials	N (%)	C (%)	S (%)	N/S
1	IE-MoS ₂ (1.0)	2.84	1.00	32.59	0.087
2	IE-MoS ₂ (1.5)	3.03	1.03	33.90	0.089
3	IE-MoS ₂ (3.0)	3.02	0.72	37.26	0.081
4	IE-MoS ₂ (6.0)	1.87	0.95	37.81	0.049
5	NE-MoS ₂ ^[b]	1.52	0.59	37.50	0.041
6	MoS ₂ -H	0.03	0.20	41.33	0.001
7	MoS ₂ -C	0.20	0.34	41.28	0.005
8	MoS ₂ -AP	2.05	0.49	34.19	0.060

^[a] The contents were determined by CHNS elemental analysis; ^[b] The NE-MoS₂ was obtained after a prolonged hydrothermal reaction for 12.0 h.

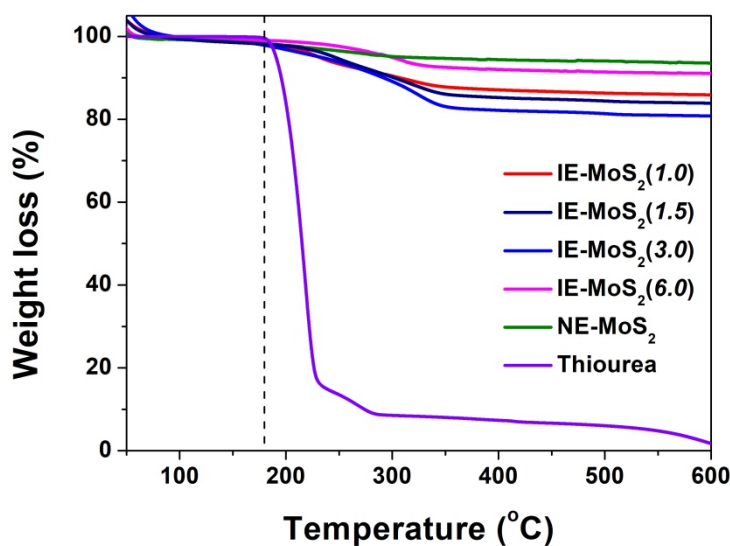


Fig. S1 TGA profile of thiourea and various MoS₂ obtained at different reaction time. The measurements were performed under a N₂ flow with a temperature ramping rate of 5 °C min⁻¹.

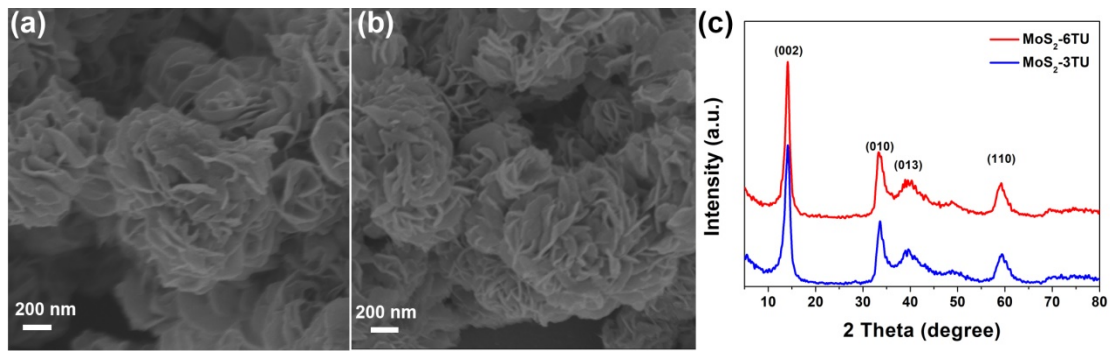


Fig. S2 SEM images of MoS₂ nanoflowers obtained with a feeding S/Mo ratio of (a) 3.0 and (b) 6.0. (c) Corresponding XRD profiles that show typical pattern of 2H-MoS₂ without expanded interlayers.

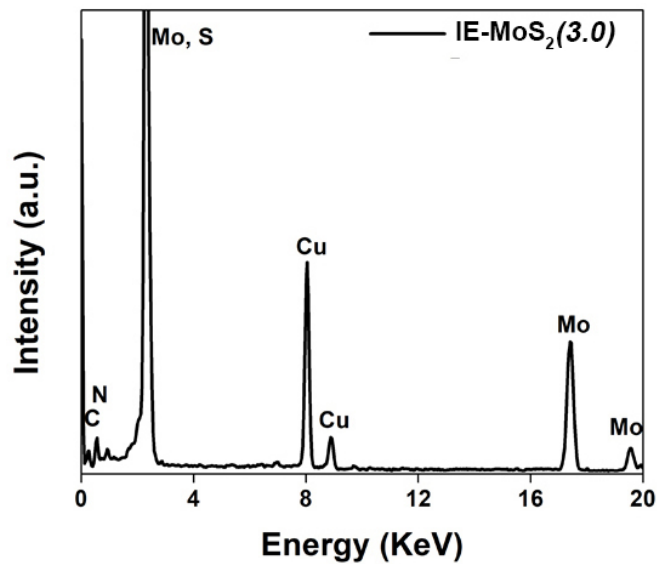


Fig. S3 EDS profile of IE-MoS₂(3.0).

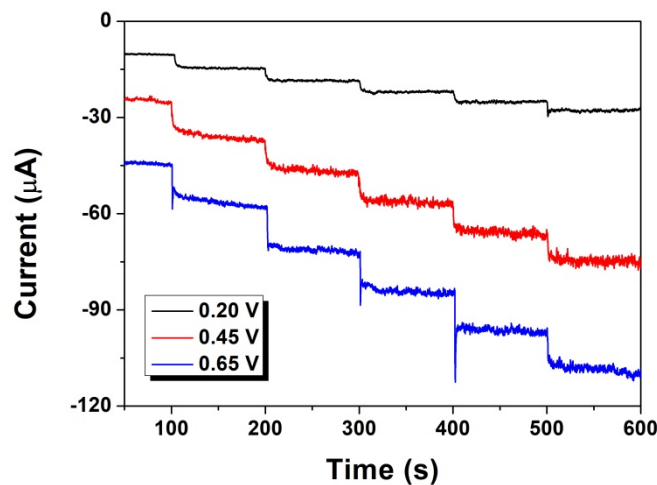


Fig. S4 Amperometric i-t curves of IE-MoS₂(3.0) in N₂-saturated PBS solution upon the successive addition of 0.1 mM H₂O₂ at different applied potential.

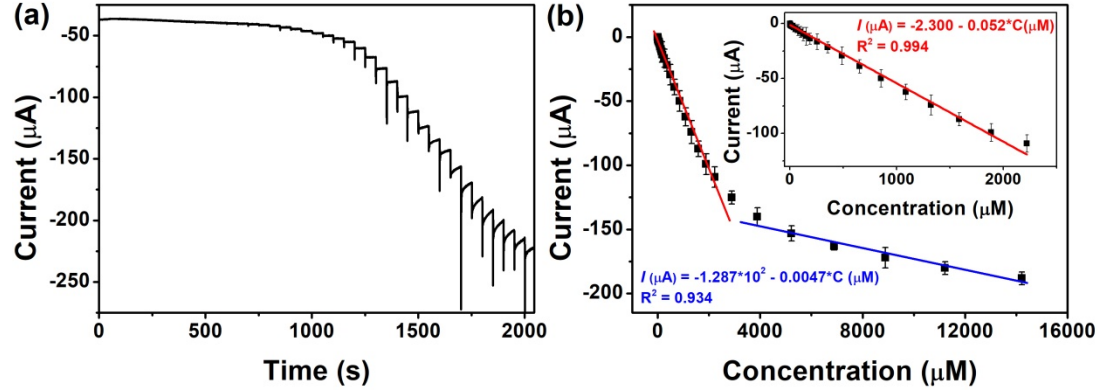


Fig. S5 (a) Amperometric response of a NE-MoS₂ modified GCE to stepwise H₂O₂ addition, and (b) calibration curve of current versus H₂O₂ concentration.

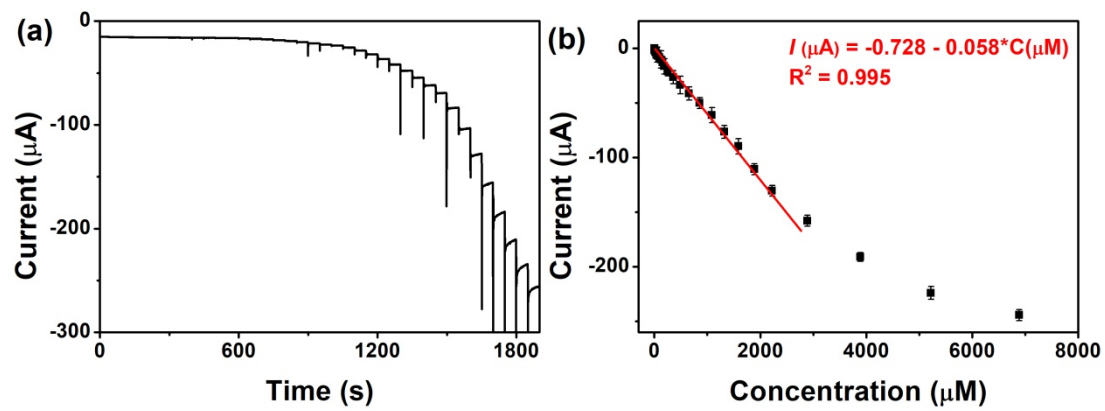


Fig. S6 (a) Amperometric response of a IE-MoS₂(1.0) modified GCE to stepwise H_2O_2 addition, and (b) calibration curve of current versus H_2O_2 concentration.

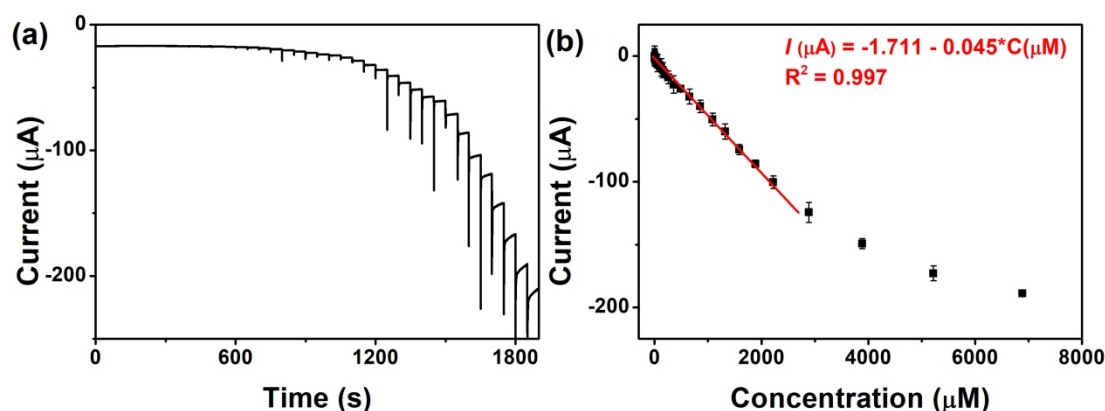


Fig. S7 (a) Amperometric response of a IE-MoS₂(1.5) modified GCE to stepwise H_2O_2 addition, and (b) calibration curve of current versus H_2O_2 concentration.

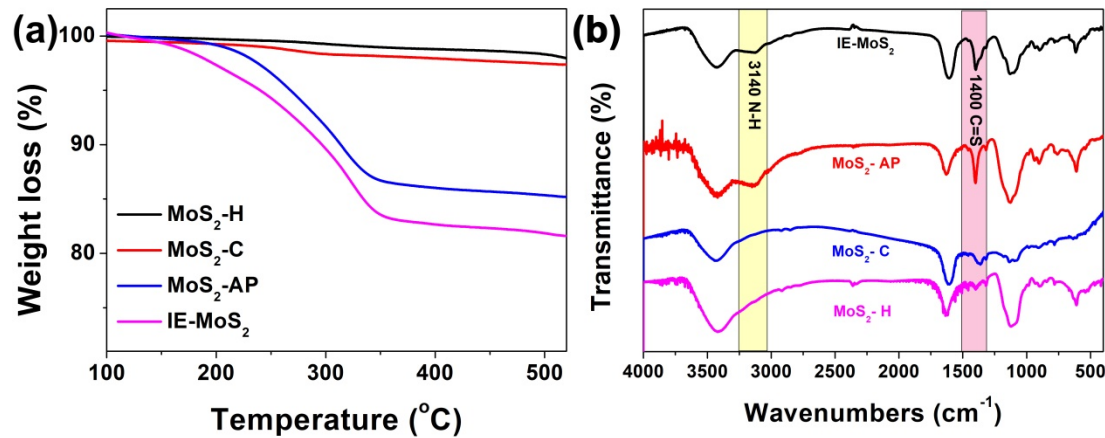


Fig. S8 (a) TGA curves and (b) FT-IR spectra of IE-MoS₂(3.0), MoS₂-C, MoS₂-H and MoS₂-AP. In the TGA profiles, the negligible loss in MoS₂-C and MoS₂-H suggests the absence of thiourea, and the considerable one on MoS₂-AP is accordant with the partially shrinking interlayers. This observation can be identical to the FT-IR analysis.

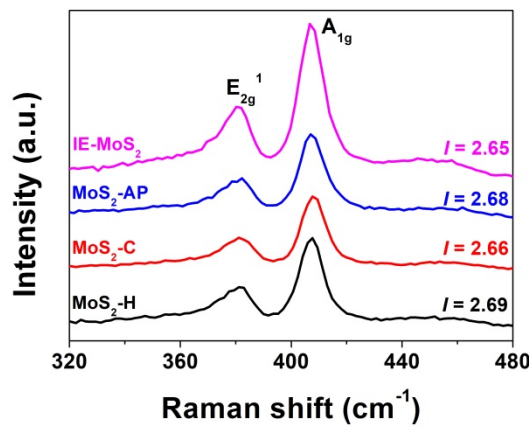


Fig. S9 Raman spectra of IE-MoS₂(3.0), MoS₂-C, MoS₂-H and MoS₂-AP. Obervably, the similar I ratio ($\text{A}_{1g}/\text{E}_{2g}^1$) indicates the well-retained edge sites after shrinking interlayers.

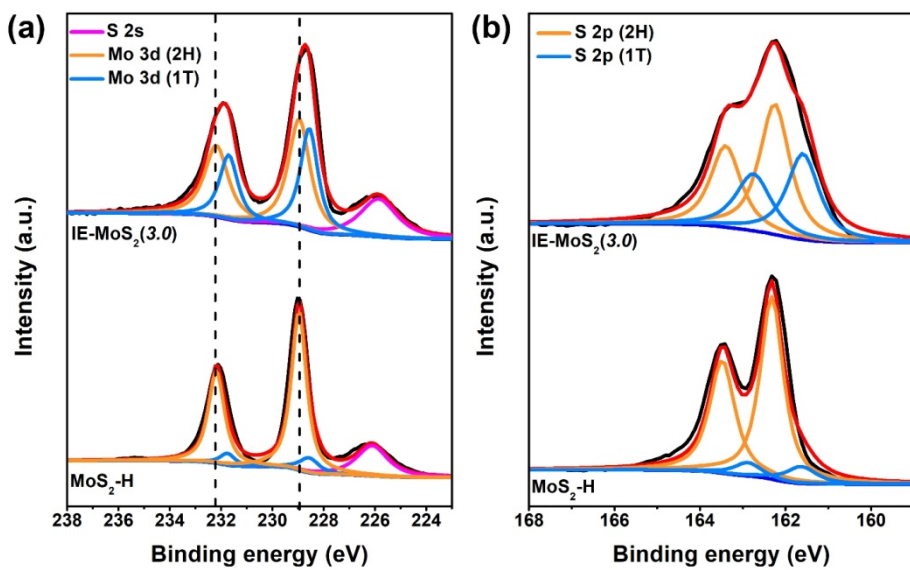


Fig. S10 XPS spectra of (a) Mo 3d and (b) S 2p in IE-MoS₂(3.0) and MoS₂-H. The IE-MoS₂(3.0) identifies a relatively higher content of 1T phase, in comparison with MoS₂-H after hydrothermal treatment by 0.05 M H₂SO₄.

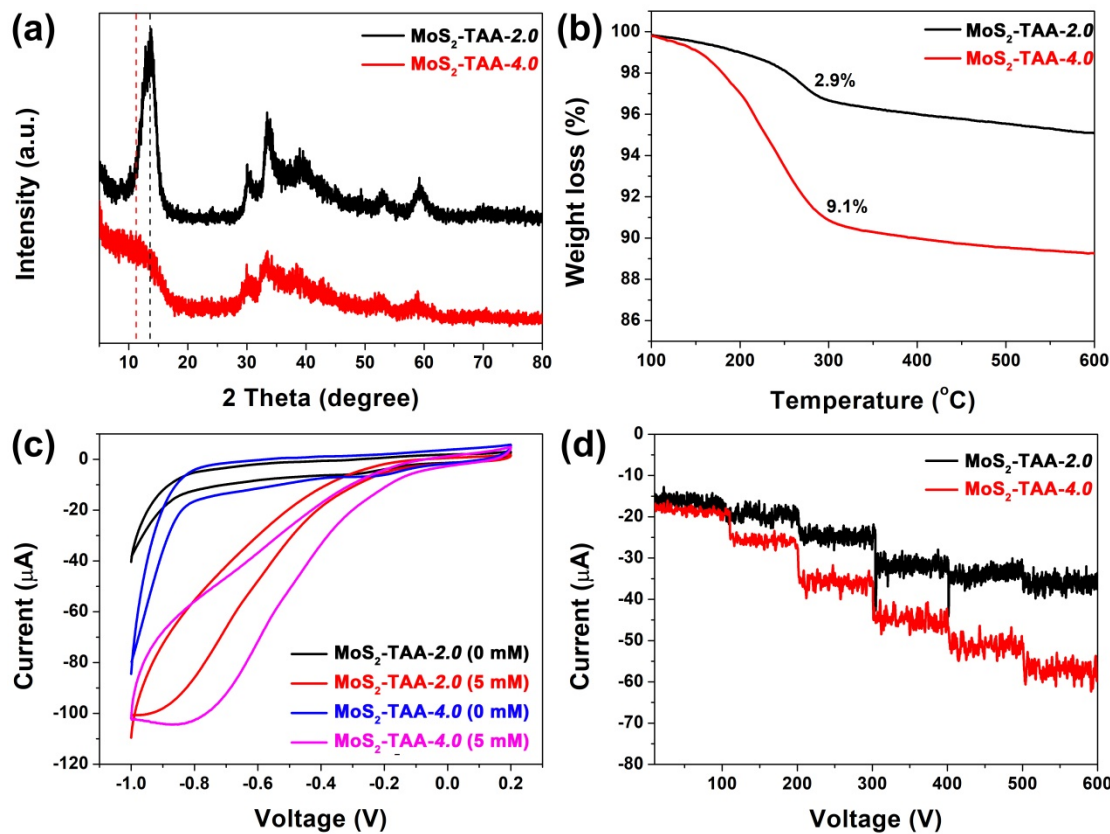


Fig. S11 Structural characterization and electrochemical sensing performance of MoS₂ prepared with TAA. According to the different feeding ratio of TAA/Mo (*n*), the as-received samples are denoted as MoS₂-TAA-*n*. (a) XRD patterns and (b) TGA curves of MoS₂-TAA-2.0 and MoS₂-TAA-4.0. The obviously expanded interlayers in MoS₂-TAA-4.0 are identified by the broad diffraction peak starting from $2\theta = 9.0^\circ$ in XRD and the obvious weight loss in TGA. (c) CVs responses and (d) Amperometric i-t curves (with successive additions of 0.1 mM H₂O₂ at -0.65 V vs. Ag/AgCl) of the above samples in N₂-saturated PBS solution upon H₂O₂ injection. The MoS₂-TAA-4.0 with expanded interlayers affords a more sensitive response to H₂O₂ in comparison with MoS₂-TAA-2.0.

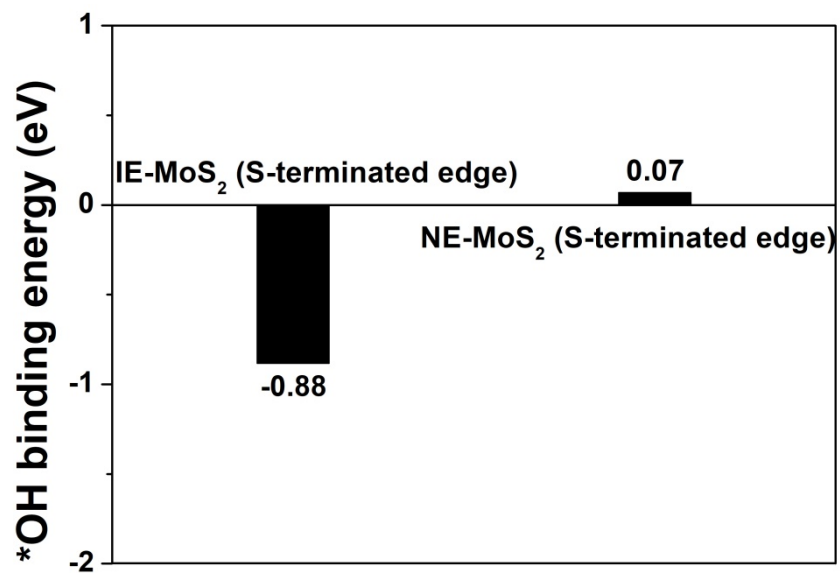


Fig. S12 Binding energy of *OH on S-terminated edge sites of IE-MoS₂ and NE-MoS₂.